

Magnetization Curves of Randomly Assembled Nanomagnets

H. Maniwa, I. Nakatani, S. Nimori, and T. Furubayashi

National Institute for Materials Science, Tsukuba 305-0047, Japan

*Corresponding author: MAM1YA.hiroaki@nims.go.jp. Phone: +81 29 859 2755, Fax: +81 29 859 2701

More than half a century ago, magnetization curves for individual nanomagnets were well explained by the Langevin function $L(x)$ in the superparamagnetic picture. We cannot, however, interpret the magnetizing processes of actual nanomagnet assemblies even in the century of nanotechnology, because thermal fluctuation, magnetic anisotropy, dipolar coupling, and exchange interaction cooperate or compete with magnetizing force from the applied field. In this work, effects of dipolar coupling in simply assembled nanomagnets without exchange interactions are examined by controlling its strength $-J_{dij} = \sum_j \mu_i \mu_j - \alpha \cdot \mu_i \cdot M_j$ in two methods, where α is a proportionality constant, μ is the total magnetization of each nanomagnet, and M_s is the saturation magnetization.

In the first method, $\text{Co}_x\text{Ag}_{1-x}$ ($x < 0.33$) nanogranular films were prepared, because only the magnitude of μ can be grown without variation of M_s by the annealing at 673 K. Then, their anisotropic magnetization curves were measured. At higher temperatures, their magnetization curves are scaled by the ratio of field to temperature H/T as ideal superparamagnets. On the other hand, their curves become independent of temperature at lower temperatures. This feature has already observed in prior works, where interacting Super-Paramagnet (ISP) scenario has been discussed. In this scenario, the dipolar coupling plays the same role with the thermal fluctuation. Hence, M/M_s is given by $L(\mu H / (T + J_{dij})) \sim L(\alpha \cdot H \cdot M_s)$ at the lower temperature $T \ll J_{dij}$. If this scenario is applicable, the temperature-independent magnetization curves of annealed film should be the same with those of the corresponding as-made films. It is, however, found that the curves become much steeper after annealing, in spite of nearly constant M_s . We know that μ increases during the annealing. Additionally, the estimated switching field distribution shows that effective anisotropy constant K_{eff} dramatically decreases during it. Therefore, the observed change of the temperature-independent magnetization curve is attributed to the increase of magnetizing force μH , or the decrease of magnetic anisotropy K_{eff} .

Minor effects of the dipolar coupling on the magnetizing processes can be confirmed by the other method, where frozen iron-nitride magnetic fluids were used. Note that only the density of nanomagnets can be controlled by its dilution in the melted state. In the present case, M_s varies from 9 to 33 emu/cm^3 without variation of $\mu \sim 10000 \mu_B$ nor of $K_{eff} \sim 5 \times 10^7 \text{ erg/cm}^3$. For the samples, we find the anisotropic magnetization curves are nearly independent of temperature below 150K. The point is that the curves of the samples with various M_s are almost superimposed on each other when M/M_s is simply plotted for H . The exceptions are only the initially magnetizing curves. In other words, the temperature-independent magnetization curve are not affected by the dipolar coupling, because its strength is proportional to M_s . For this reason, we can conclude that the magnetizing process of these assembled nanomagnets at the low temperatures is a rotation magnetization dominated by the competition between the magnetic anisotropy of each nanomagnet and the magnetizing force from the applied field.

REFERENCE

[1] P. Altia, M. Coisson, P. Tiberto, F. Vinai, M. Knobel, M. A. Novak, and W. C. Nunes, Phys. Rev. B 64, 144420 (2001).

Etch Characteristics of Magnetic Tunnel Junction Stack Using a High Density Plasma in a HBr/Ar Gas

Su Ryun Min¹, Han Na Cho¹, Seung Pil Choi¹, Jung Seung Kim²,
Kyung Ho Shih², and Chee Won Chung^{*1}

¹Department of Chemical Engineering, INHA University, 253 Yonghyun-Dong, Nam-Gu, Incheon, 402-751, Korea
²Nano-Device Research Center, Korea Institute of Science and Technology, 39-1 Hawolgok-Dong, Seongbuk-Gu, Seoul, 136-791, Korea

*Corresponding author: cwchung@inha.ac.kr. Phone: +82 32 860 7473, Fax: +82 32 872 0959



Fig. 1. Etched MTJ stack at (a) pure Ar, (b) 10% HBr and (c) 20% HBr in HBr/Ar. The MTJ size: 300x 400nm².

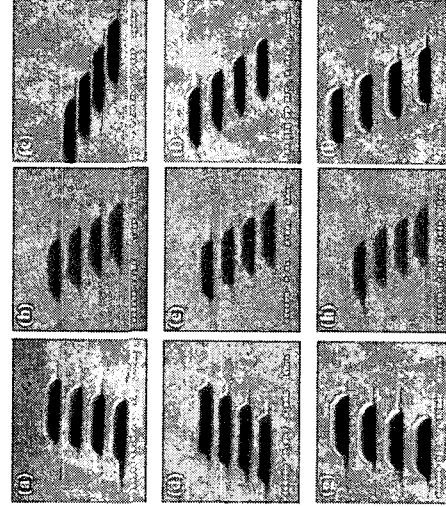


Fig. 2. Etched MTJ stack varying coil rf power of (a) 700 W, (b) 900 W, and (c) 1000 W, dc-bias voltage of (d) 200 V, (e) 300 V, and (f) 400 V, and gas pressure of (g) 1 mTorr, (h) 5 mTorr, and (i) 10 mTorr. Etch gas: HBr/Ar. The MTJ size: 300x 400nm².

profile. A high degree of anisotropic etching of MTJ stack was achieved using Cl_2/Ar gas at the optimized etching conditions.

REFERENCES

[1] B. Shim, Y. S. Song, S. J. Park, T. W. Kim, and C. W. Chung, phys. stat. sol. (a), 201, 1644 (2004).

Recently, magnetic random access memory (MRAM), based on magnetic tunnel junction (MTJ) stack and CMOS, has a great attention as a prospective semiconductor due to nonvolatility, fast access time, unlimited read/write endurance, low operating voltage, and high storage density [1]. The etching of MTJ stack is one of the important processes for the realization of high density MRAM devices.

The etch characteristics of MTJ stack are investigated using an inductively coupled plasma reactive ion etcher in a HBr/Ar gas mixture. Since the MTJ stack which consists of various magnetic materials, metals, and a tunneling barrier layer rarely reacted with chemical species in a plasma, TiN thin film was employed as a hard mask for etching of MTJ stack. For the fabrication of 256 M-level MRAMs, the MTJ stack with TiN hard masks were patterned with nanometer-size (300 nm x 400 nm) using an electron-beam lithography process. Firstly, TiN hard masks were etched in a $\text{Cl}_2/\text{C}_2\text{F}_4/\text{Ar}$ plasma, and then MTJ stacks were etched on varying HBr gas concentration and etch parameters including coil rf power, dc-bias voltage and gas pressure.

Etch characteristics of MTJ stack was examined by varying HBr concentration. As HBr concentration increased, the etch profile of MTJ stack etched at 20% HBr was better than the others in Fig. 1.

Etch characteristics of MTJ stack were investigated by varying etch parameters including coil rf power, dc-bias voltage and gas pressure. The etch slope of etched MTJ stack at low coil rf power and dc-bias voltage, became more vertical. The MTJ stack etched at high gas pressure had better etch